BMJ Open Respiratory Research

Protective role of the HSP90 inhibitor, STA-9090, in lungs of SARS-CoV-2-infected Syrian golden hamsters

Luiz Gustavo Teixeira Alves ,[1] Morris Baumgardt,[2] Christine Langner,[3] Mara Fischer,[2] Julia Maria Adler,[3] Judith Bushe,[4] Theresa Catharina Firsching,[5] Guido Mastrobuoni,[6] Jenny Grobe,[6] Katja Hoenzke,[2] Stefan Kempa,[6] Achim Dieter Gruber,[5] Andreas Christian Hocke,[2] Jakob Trimpert,[3] Emanuel Wyler,[1] Markus Landthaler[1,7]

To cite: Teixeira Alves LG, Baumgardt M, Langner C, *et al*. Protective role of the HSP90 inhibitor, STA-9090, in lungs of SARS-CoV-2-infected Syrian golden hamsters. *BMJ Open Respir Res* 2024;**11**:e001762. doi:10.1136/bmjresp-2023-001762

► Additional supplemental material is published online only. To view, please visit the journal online (https://doi.org/10.1136/bmjresp-2023-001762).

Received 13 April 2023
Accepted 26 January 2024

For numbered affiliations see end of article.

Correspondence to
Dr Luiz Gustavo Teixeira Alves;
gustavo.teixeira@mdc-berlin.de

ABSTRACT

Introduction The emergence of new SARS-CoV-2 variants, capable of escaping the humoral immunity acquired by the available vaccines, together with waning immunity and vaccine hesitancy, challenges the efficacy of the vaccination strategy in fighting COVID-19. Improved therapeutic strategies are urgently needed to better intervene particularly in severe cases of the disease. They should aim at controlling the hyperinflammatory state generated on infection, reducing lung tissue pathology and inhibiting viral replication. Previous research has pointed to a possible role for the chaperone HSP90 in SARS-CoV-2 replication and COVID-19 pathogenesis. Pharmacological intervention through HSP90 inhibitors was shown to be beneficial in the treatment of inflammatory diseases, infections and reducing replication of diverse viruses.

Methods In this study, we investigated the effects of the potent HSP90 inhibitor Ganetespib (STA-9090) in vitro on alveolar epithelial cells and alveolar macrophages to characterise its effects on cell activation and viral replication. Additionally, the Syrian hamster animal model was used to evaluate its efficacy in controlling systemic inflammation and viral burden after infection.

Results In vitro, STA-9090 reduced viral replication on alveolar epithelial cells in a dose-dependent manner and lowered significantly the expression of proinflammatory genes, in both alveolar epithelial cells and alveolar macrophages. In vivo, although no reduction in viral load was observed, administration of STA-9090 led to an overall improvement of the clinical condition of infected animals, with reduced oedema formation and lung tissue pathology.

Conclusion Altogether, we show that HSP90 inhibition could serve as a potential treatment option for moderate and severe cases of COVID-19.

WHAT IS ALREADY KNOWN ON THIS TOPIC

⇒ COVID-19 still causes a high burden of disease worldwide, with substantial number of deaths. Efficient therapeutics are, therefore, still needed to treat severe cases of COVID-19.

WHAT THIS STUDY ADDS

⇒ HSP90 inhibition with STA-9090 (ganetespib) showed antiviral and anti-inflammatory capacities in vitro and tissue protective features in a hamster model of COVID-19.

HOW THIS STUDY MIGHT AFFECT RESEARCH, PRACTICE OR POLICY

⇒ The use of STA-9090, already in phase III studies in a diverse spectrum of diseases, may be efficient against COVID-19 and should be considered as potential therapeutic to treat the disease.

INTRODUCTION

The COVID-19 is a global threat with over 750 million people infected by the causal agent of the disease, the beta-coronavirus SARS-CoV-2. Since the beginning of the pandemic, nearly 7 million deaths have been reported worldwide.[1 2] Infections lead mostly to mild to moderate symptoms or remain asymptomatic. However, in some cases, the disease can progress to severe acute respiratory distress syndrome (ARDS), with increased lung injury and oedema formation in the lungs, being associated with high mortality rates.[2–4] Dysregulated systemic and mucosal immune responses, elevated proinflammatory cytokine levels, and robust activation of the coagulation cascade, are frequently observed manifestations of the disease.[4–6] Pre-existing comorbidities, such as diabetes, were correlated with a higher likelihood of developing more severe cases of the disease and a higher mortality rate. This is probably due to an impaired immunological response to the virus.[4 7] Within the lungs, epithelial cells are the main cell type expressing the viral entry factor ACE2 and are promptly infected by SARS-CoV-2.[8] Although endothelial cells are likely only barely susceptible to SARS-CoV-2 infection, they are affected by the local inflammation.[9 10] This may lead to cell dysfunction,

cell death and the deterioration of barrier functions, characteristic of ARDS.[9 11] In severe cases of COVID-19, antiviral drugs may not be sufficient to ameliorate patient's conditions, as a systemic inflammation may have already been established. The administration of glucocorticoids, targeting the uncontrolled hyperinflammation, has been evaluated for its efficacy in reducing disease severity.[12 13] However, positive effects were mostly observed among patients receiving respiratory support.[14 15]

The activation of inflammatory responses with production of cytokines and chemokines, which contribute to immune cell recruitment and tissue inflammation, is partially regulated by heat-shock proteins (HSPs).[16] HSPs constitute a large family of chaperones that assist the nascent polypeptide chain to undergo functional conformation changes, promoting its stabilisation, necessary for protein localisation and function.[17 18] HSP90 is crucial for the maturation of proteins involved in various cellular processes, including cell division and differentiation, apoptosis and signalling events.[16 17] It has a broad range of substrates, including tyrosine-kinase receptors (eg, EGFR, c-Kit, MEK), signal-transduction proteins (eg, IKK, RAF1, N-RAS), cell-cycle regulatory proteins and transcription factors.[18 19] The NF-κB protein members, critical in inflammatory signalling pathway, cell proliferation and immune regulation, are important candidate targets of HSP90 and are promptly affected by its inhibition. Moreover, their activation depends on factors also affected by HSP90 inhibition, as IKK.[20 21] For its crucial role in stability and function of many oncogenic proteins, pharmacological intervention through HSP90 inhibitors was shown to be beneficial in a wide spectrum of tumour treatment.[18 19 22] Targeting HSP90 was also evaluated in a diverse range of diseases, including neurodegenerative[23] and inflammatory diseases,[24] and infections.[25] On infections, cell surface receptors are activated, increasing activity of RhoA. This leads to myosin light chain phosphorylation, increasing actin filament contractile forces and increased vascular permeability. Moreover, RhoA activation induces the NF-κB pathway, triggering further inflammation. As a consequence, endothelium damage and hyperpermeability occurs. HSP90 inhibition affects RhoA activation, leading to barrier protective functions on pulmonary arterial endothelial cell.[26–28] Moreover, it contributes to a reduction in inflammation, being useful as a therapeutic strategy in ARDS and other pulmonary inflammatory diseases.[24 29 30] Viruses depend on the host cell machinery for protein stabilisation and activation, which regulates the viral life cycle.[31] HSP90 inhibition was shown to affect the synthesis of important viral transcripts in vitro and is, therefore, being tested as antiviral drug in different studies.[25 29 32] We recently showed an upregulation of HSP90 transcripts in lung epithelial cells infected with SARS-CoV-2.[33] HSP90 inhibition suppressed SARS-CoV-2 replication in vitro, similarly to SARS-CoV and MERS-CoV, by a proteasome-dependent degradation of the structural protein N.[31 34 35] Moreover, HSP90 inhibition prevented endothelial dysfunction and the inflammation caused by SARS-CoV-2 infection.[10 36] Therefore, this could be a possible valuable strategy to prevent lung pathology during COVID-19.

The development of novel therapeutic strategies to better intervene in severe cases of COVID-19 is urgently needed. Here, we analyse the effects of the HSP90 inhibitor STA-9090 in vitro on cell activation and viral replication. In the Syrian hamster COVID-19 model, we evaluate its efficacy in controlling systemic inflammation and the viral burden after infection. In vitro, STA-9090 application reduced viral replication on alveolar epithelial cells (AECs) in a dose-dependent manner and lowered significantly the expression of proinflammatory genes in AECs and alveolar macrophages. In vivo, STA-9090 led to an overall improvement of the clinical condition of infected animals, with reduced oedema formation and tissue pathology.

MATERIAL AND METHODS

Patient and public involvement

Patients and public were not involved in the design and development of this study.

Virus culture

SARS-CoV-2 isolate (BetaCoV/Germany/BavPat1/2020) was kindly provided by D. Niemeyer and C. Drosten, from Charité - Berlin, Germany. SARS-CoV-2 isolate was prepared as previously.[37] Integrity of the furin cleavage site was confirmed through sequencing of stocks prior to infection.

Cell culture

Vero E6 cells (ATCC CRL-1586) were cultivated in Dulbecco's modified Eagle's medium supplemented with 10% heat-inactivated fetal calf serum, 1% non-essential amino acids, 1% L-glutamine and 1% sodium pyruvate (all Thermo Fisher Scientific, USA), at 37°C. AECs were isolated from distal lung tissue and cultured as previously described.[33] Alveolar macrophages were isolated from lung biopsies performed in patient with lung tumour, as previously described.[38] Cells were incubated with virus for 1 hour at 37°C, and further treated with STA-9090. AECs were treated for 16 hours with different concentrations of STA-9090, ranging from 12.5 nM to 800 nM in a log2 scale and alveolar macrophages were treated for 24 hours with 100 nM of this inhibitor. The control group was treated with the highest concentration of the diluent DMSO. Cytotoxicity (LDH Cytotoxicity Detection Kit, Takara, Japan) and Viability test (CellTiter-Glo Luminescent Assay, Promega, USA) were performed on AECs after STA-9090 application, according to manufacturer's protocol.

Animal model

Infection was performed with 1×10^5 PFU SARS-CoV-2 diluted in 60 µL MEM, applied intranasally (i.n.) in

the hamsters, as previously described.[37] In the first in vivo experimental set, Syrian hamsters were randomly assigned to three groups, all being infected. The intraperitoneal (i.p.) treatment with 25 mg/kg body-weight of STA-9090 (kindly provided by Aldeyra Therapeutics, USA) was performed together with infection at day 0 (group 1) or twice, both at day 0 and day 4 post-infection (p.i.) (group 2). The third group received placebo therapy. In a second experimental set, the control group received placebo treatment at day 3 after infection, while other two groups received STA-9090 at 48 hours or 72 h p.i. Animals are depicted for sex in online supplemental table 1. Animals included in the experiment were monitored for signs of disease twice daily, with weight and temperature measured for compliance with score sheet criteria. Serum, EDTA blood, oropharyngeal swabs and lungs were collected for virologic, histopathological and sequencing analysis.

Viral load quantification

Virus titers and RNA copies were determined by plaque assay and quantitative RT-PCR analysis as previously described.[37] Analysis was performed in oropharyngeal swabs and from homogenised lung tissue.

Histopathology for SARS-CoV-2-infected hamsters

Lungs were embedded in paraffin and sections were made from tissue for immunostaining and analysis. Lung tissue pathology was evaluated by board-certified veterinary pathologists in a blinded fashion following standardised recommendations, including pneumonia-specific scoring parameters as described previously.[37]

Bulk RNA analysis

Sequencing was performed on total RNA isolated from AECs, alveolar macrophages and blood samples using Trizol reagent. Libraries were constructed using the NEBNext Ultra II Directional RNA Library Prep Kit (New England Biolabs, USA) and sequenced on a high throughput NextSeq 500 device (Illumina, USA). Reads were aligned to the human reference genome hg38 (GRCh38) or the Syrian hamster genome (MesAur1.0) using hisat2.[39] Gene expression was quantified using the package featureCounts from Rsubread[40] and analysed by DESeq2.[41]

Mass spectrometry

Serum and lung samples were prepared with RIPA lysis buffer. Samples were extracted by mixing 25 µL of sample with 25 µL of 25% w/w acetonitrile (ACN) in water, 100 µL of formic acid 0.1% and 400 µL of methyl-t-butyl ether (MTBE). Samples were centrifuged at 3000×g and supernatant collected for new extraction with 400 µL of MTBE. Both extracted supernatants were pooled dried under nitrogen and resuspended in 50 µL of 40% ACN in water before analysis. Samples were analysed on a Quantiva triple quadrupole (Thermo Fisher Scientific, USA) coupled to a 1290 Infinity HPLC (Agilent Technologies, USA), using a Zorbax Eclipse column (2.1×50 mm, 1.8 µm particle size). Separation was performed using a 0.3 mL/min gradient ranging from 40% of solvent B (acetonitrile with 0.1% formic acid; solvent A=water with 0.1% formic acid) to 95% in 2 min. The HESI source was operated with 3500 V spray voltage, 30 arbitrary units sheat gas, 8 arbitraty units auxiliary gas and 350°C transfer tube and vaporiser temperature. Two transitions were monitored (365 ->131 and 365 ->323) in positive mode. Quantification was performed using QuanBrowser software (Thermo Fisher Scientific, USA).

Western blot

Lung tissue homogenate was assessed to verify expression of HSP90 and phospho-HSP90 protein levels. β-actin was used as internal control. Antibodies against HSP90 (Abcam, UK), phospho-HSP90 (Thermo Fisher Scientific, USA) and β-actin (Sigma Aldrich, USA) were used as primary antibodies. Secondary antibodies conjugated to HRP against rabbit (Agilent Technologies, USA) or mouse (Agilent Technologies, USA) were used. Protein presence was visualised with an Amersham Imager 680 (GE Healthcare, USA) with the chemiluminescent-based ECL western blotting detection reagents (Cytiva, Sweden).

Statistical analysis

GraphPrism V.9.1.2 software (GraphPad Software, USA) was used for statistical analysis of the clinical data and quantification of virus titers. Details of statistical analysis are described at the figure legend of each experiment. One-way or two-way analysis of variance with Tukey's multiple comparisons test for unpaired data was used for the in vivo data. Unpaired t-test was used to compare PFU counting of AECs. Further data on viral replication were compared using Mann-Whitney U test. P values are shown as following for significance: $p<0.05$ (*), $p<0.01$ (**).

RESULTS

STA-9090 has antiviral and anti-inflammatory properties in AECs and alveolar macrophages

Distinct viruses depend on HSP90 to replicate. The hepatitis C virus depends on HSP90 for the activity of the NS2/3 protease, essential for RNA replication. Gastroenteritis virus, porcine epidemic diarrhoea virus and swine acute diarrhoea syndrome-CoV depend on the constitutively expressed isoform HSP90β for virion assembly. While dengue virus depends on the isoform HSP90α, normally stress-induced, for cellular entry.[42 43] SARS-CoV-2 also depends on HSP90, as its inhibition led to a reduction on replication in Calu-3 lung epithelial cells and AECs.[33 36] To evaluate the properties of STA-9090 on differentiated AECs, we infected cells with an MOI

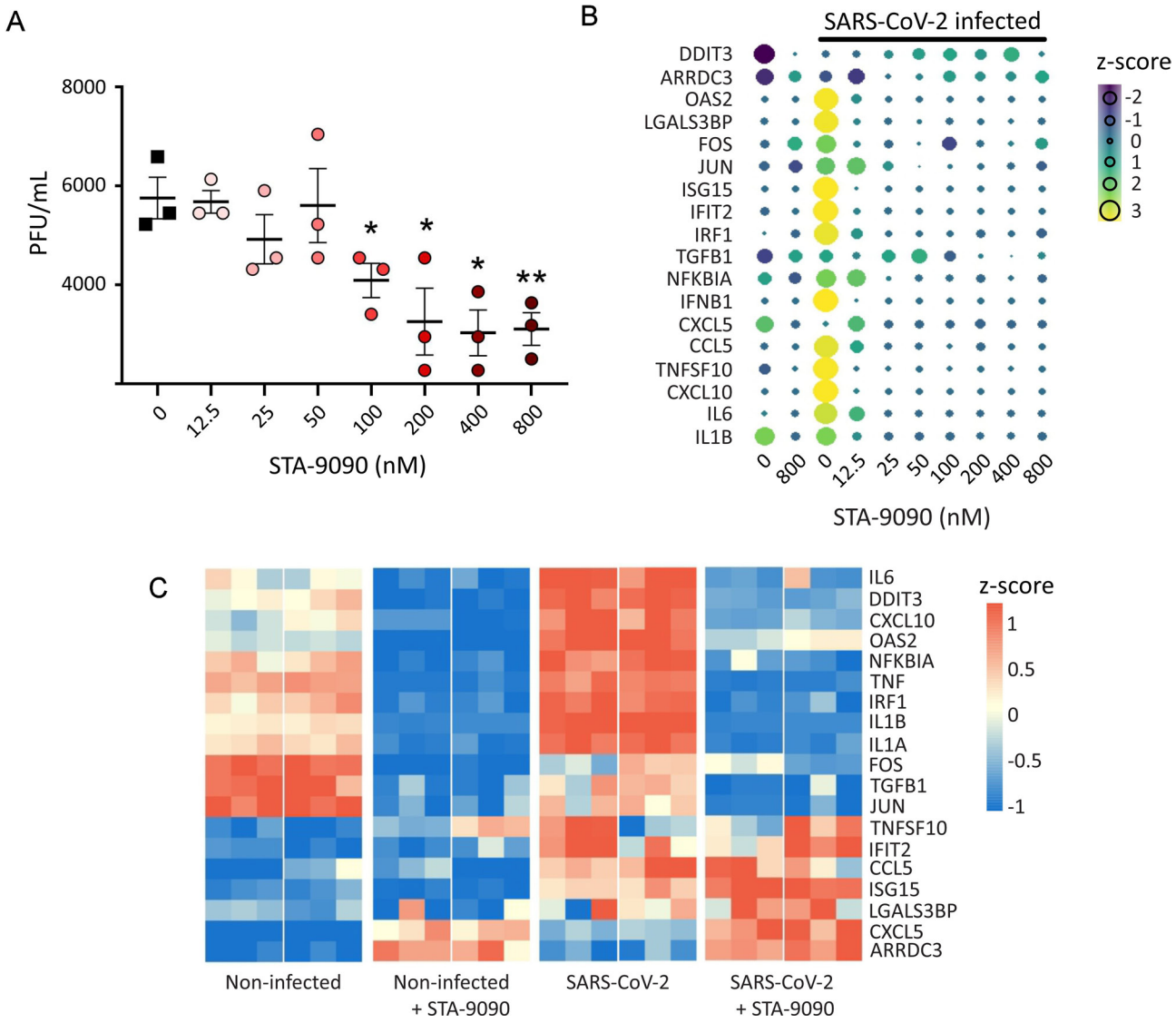

Figure 1 Antiviral and anti-inflammatory properties of STA-9090 in vitro in infected AECs and alveolar macrophages. AECs, isolated from human lung tissue, were infected with MOI 0.5 of SARS-CoV-2 and treated with different concentrations of the HSP90 inhibitor STA-9090. STA-9090 concentrations ranged from 12.5 nM to a maximum of 800 nM on a log2 scale. Non-treated or non-infected cells serve as control. (A) Viral titers in supernatants of AECs infected with SARS-CoV-2 and treated with the indicated concentration of STA-9090. (B) Expression analysis of selected induced genes in AECs. Shown are z-scores of DESeq2 normalised counts comparing infected samples to uninfected control samples mock-treated or treated with different concentrations of STA-9090, as shown. Size of the circle and colours show differentiated expression. Alveolar macrophages were differentiated from lung tissue and infected with SARS-CoV-2 (MOI 0.5) prior to treatment with STA-9090. Mock infected cells, treated or non-treated, served as control. (C) Heatmaps of differently expressed genes in alveolar macrophages after infection with SARS-CoV-2 and treatment with 100 nM STA-9090. Uninfected cells, receiving STA-9090 or not, were used as controls. Genes related to IFN-mediated signalling pathway, type I IFN signalling, cellular-response to IFNγ and cytokines were selected, as previously described.[60] Columns represent samples and rows genes. Shown are z-scores of DESeq2-normalised data from two donors, analysed independently and colour scale ranges from blue (10% lower quantile) to red (10% upper quantile) of the selected genes. N=3 in A, C and n=2 in B. Unpaired t-test used for comparison in A. *p<0.05, **p<0.01. AECs, alveolar epithelial cells.

of 0.5 of SARS-CoV-2, and treated them with different concentrations of this inhibitor, ranging from 12.5 nM to 800 nM. As shown previously,[43–45] STA-9090 did not show any sign of cytotoxicity towards the cells (online supplemental figure 1A). Similar to other HSP90 inhibitors, STA-9090 led to a statistically significant inhibition in viral replication at concentrations equal or higher than 100 nM (figure 1A). On infection of lung epithelial cells with SARS-CoV-2, an inflammatory response is initiated, with upregulation of the NF-kB signalling response and the expression of specific inflammatory cytokines.[46] Increased release of proinflammatory cytokines, as TNFα, IL-1β and IL-6 are associated with increased organ damage during COVID-19.[31] To further examine the

role of STA-9090 on inflammation, we performed RNA sequencing from infected AECs. Expression of proinflammatory cytokines, including IL-6, IL-1b, CXCL10, CCL5 and TNFSF10, enhanced on infection, was reduced by the treatment with STA-9090. This reduction was already observed with the lowest concentration of STA-9090 used. In addition, expression of NFKBIA, IFNγ-related genes and genes induced by type I IFN response, including IFIT2 and IRF1, was reduced by the treatment, when comparing to untreated infected cells. Cellular stress markers, including ARRDC3, DDIT3, JUN and FOS, were neither affected by infection, nor by the treatment. STA-9090 treatment alone did not alter expression of the inflammatory markers described (figure 1B).

Monocytes and macrophages were suggested to be critical mediators of the inflammatory responses in COVID-19, contributing to tissue pathology.[47] Alveolar macrophages were shown to take up SARS-CoV-2 without productive replication, leading to an activation of the inflammatory and antiviral pathways, contributing to lung tissue pathology.[48] To characterise the effect of STA-9090 on alveolar macrophages, RNA sequencing was performed after infection of cells with an MOI of 0.5 of SARS-CoV-2 and treatment with STA-9090. Treatment of non-infected alveolar macrophages showed no sign of cellular activation, with an overall low expression of cytokines, IFN-related genes and stress markers. Infection with SARS-CoV-2 led to an increase in expression of proinflammatory markers, as IL6, NFKBIA, TNF, IL1A, which were strongly reduced after treatment with STA-9090. Similar to AECs, expression of distinct cytokines, genes belonging to the IFNγ response and to type I IFN response, including interferon regulatory factors and interferon stimulated genes, were reduced after treatment with STA-9090, with values comparable to uninfected cells (figure 1C and online supplemental figure 1B).

Administration of STA-9090 on infected hamsters does not affect pulmonary viral loads

On SARS-CoV-2 infection, Syrian hamsters present a moderate course of COVID-19 with strong immune cell influx in the lungs, pulmonary inflammation and lung tissue pathology.[37] To assess the antiviral and anti-inflammatory properties of STA-9090 in vivo, Syrian hamsters were infected with 1×10^5 PFU SARS-CoV-2 and treated with this inhibitor (figure 2A). Infection led to a progressive decrease of body weight, as observed previously,[37] which was not altered by administration of STA-9090 (figure 2B). Viral loads were quantified from homogenised lung tissue and oropharyngeal swabs (figure 2C) by RT-qPCR, and plaque assays were performed on the lung tissue homogenate (online supplemental figure 2A). Virus was detected in both compartments and virus titers decreased over time, with undetectable levels 7 days p.i. Treatment with STA-9090 did not affect viral loads in the lung tissue and swabs, as determined by RT-qPCR and plaque assay. In vitro, STA-9090 could reduce viral loads in AECs with concentrations equal or higher than 100 nM. To quantify the concentration of STA-9090 in the Syrian hamsters, mass spectrometry was performed on lung homogenates and serum of the animals at days 1, 3, 5 and 7 after STA-9090 administration. One-day post-treatment, concentrations of STA-9090 in lungs ranged from 10 to 15 nM, and in serum of about 6 nM. STA-9090 concentrations decreased progressively with time, with almost non-detectable levels 5 days after treatment (figure 2D).

STA-9090 reduces lung pathology in infected Syrian hamsters

Lung tissue histology was examined on longitudinal sections of the left lobes of the lungs of infected hamsters after treatment with STA-9090. Infected tissue presented increased infiltration of immune cells and formation of oedema, as seen by the histology of the whole tissue. Analysis of the epithelial cell layer and the alveolar space, including the endothelial cell layer, showed increased cell hyperplasia and inflammation after infection. Treatment with STA-9090 was sufficient to reduce tissue pathology and inflammation, when comparing to the untreated control group (figure 3A). Tissue analysis by semiquantitative scores shows that the treatment with STA-9090 led to a significant reduction on lung affected area among animals of group 2 at day 7 p.i. Reduced endotheliitis was observed among animals receiving twice STA-9090 at day 5 p.i., in comparison to the other groups (figure 3B). Inflammation and perivascular oedema formation (online supplemental figure 2B), alveolar oedema and alveolar epithelial type 2 (AT2) cell hyperplasia (figure 3C) presented an apparent, but not significant, reduction in the score levels after treatment. Alveolar epithelial necrosis, bronchitis (online supplemental figure 2C) and immune cell infiltration, including lymphocytes, macrophages and neutrophils (online supplemental figure 2D), showed no differences among the groups. However, STA-9090 treatment led to a significant decrease in broncho-epithelial hyperplasia among animals receiving twice STA-9090, compared with the control group (online supplemental figure 2C). Western blot targeting HSP90 and its phosphorylated version were performed on lung tissue homogenate to investigate possible effects of HSP90 inhibition on phosphorylation. No differences were seen in the ratio of phospho-HSP90 to total HSP90, when comparing to uninfected animals (online supplemental figure 2E).

Late application of STA-9090 reduces lung inflammation in infected Syrian hamsters

To better translate to the actual treatment course in patients, we repeated the infection experiments of Syrian hamsters with a later application of STA-9090. Infected hamsters receiving Mock treatment (GB control) or

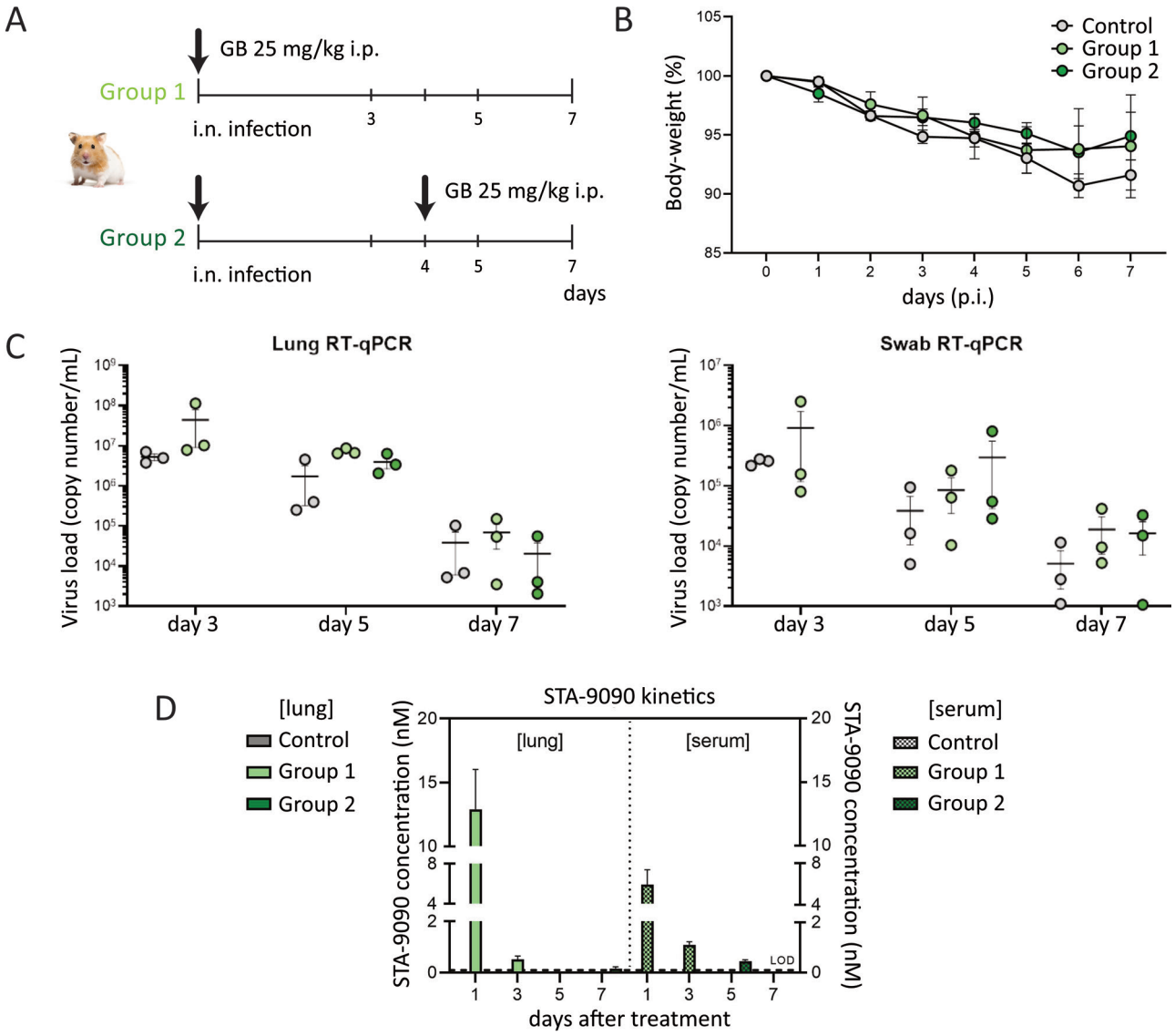

Figure 2 Treatment with STA-9090 does not affect viral loads in Syrian hamsters. (A) Syrian hamsters challenged with SARS-CoV-2 (1×10^5 PFU), were treated with 25 mg/kg STA-9090 (GB) once, together with infection (group 1), or twice, at day 0 and at day 4 p.i. (group 2). Control group received same volume of dilutor at day 0 p.i. Analysis was made at day 3 (only for the control group and group 1), day 5 and day 7 p.i. (B) Body weight in percentage from the original weight was measured daily after infection of the animals with SARS-CoV-2. (C) Viral load was quantified by RT-qPCR analysis of viral genomic RNA (gRNA) copies detected in homogenised lung tissue and oropharyngeal swabs at days 3, 5 and 7 p.i. (D) Pharmacokinetics of STA-9090 quantified by mass spectrometry in the lung tissue or serum of Syrian hamsters infected with SARS-CoV-2. Shown is the number of days after STA-9090 application (first or second doses) in lung (left) and serum (right). Results are displayed as mean±SE and n=3. Comparisons were made with a one-way ANOVA test. ANOVA, analysis of variance. LOD, limit of detection.

STA-9090 at day 2 (GB 48 hours) or 3 p.i. (GB 72 hours) were analysed on day 5 p.i. (figure 4A). No significant weight loss differences were observed after treatment of the infected animals with STA-9090, comparing to the control group (online supplemental figure 3A). Concentrations of STA-9090 in lung homogenate and serum were measured at day 5 p.i., representing day 3 (GB 48 hours) or 2 (GB 72 hours) after treatment. STA-9090 concentrations in the lungs were below 10 nM 2 days after application (GB 72 hours), and slightly lower 3 days after application. In serum, similar values were observed among animals receiving STA-9090 48 h p.i., while in the second group it was not detectable (online supplemental figure 3B). RT-qPCR analysis of the lung tissue shows an increase in the viral burden in both animal groups treated with STA-9090, in comparison to mock-treated animals (figure 4B). This increase in viral titers after treatment was not observed in the plaque assay of lungs or by RT-qPCR of swabs of infected animals (online supplemental figure 3C). Histology of the lung tissue was also performed for characterisation of tissue damage and cellular infiltration (figure 4C). Overall, the area of the lungs affected by the

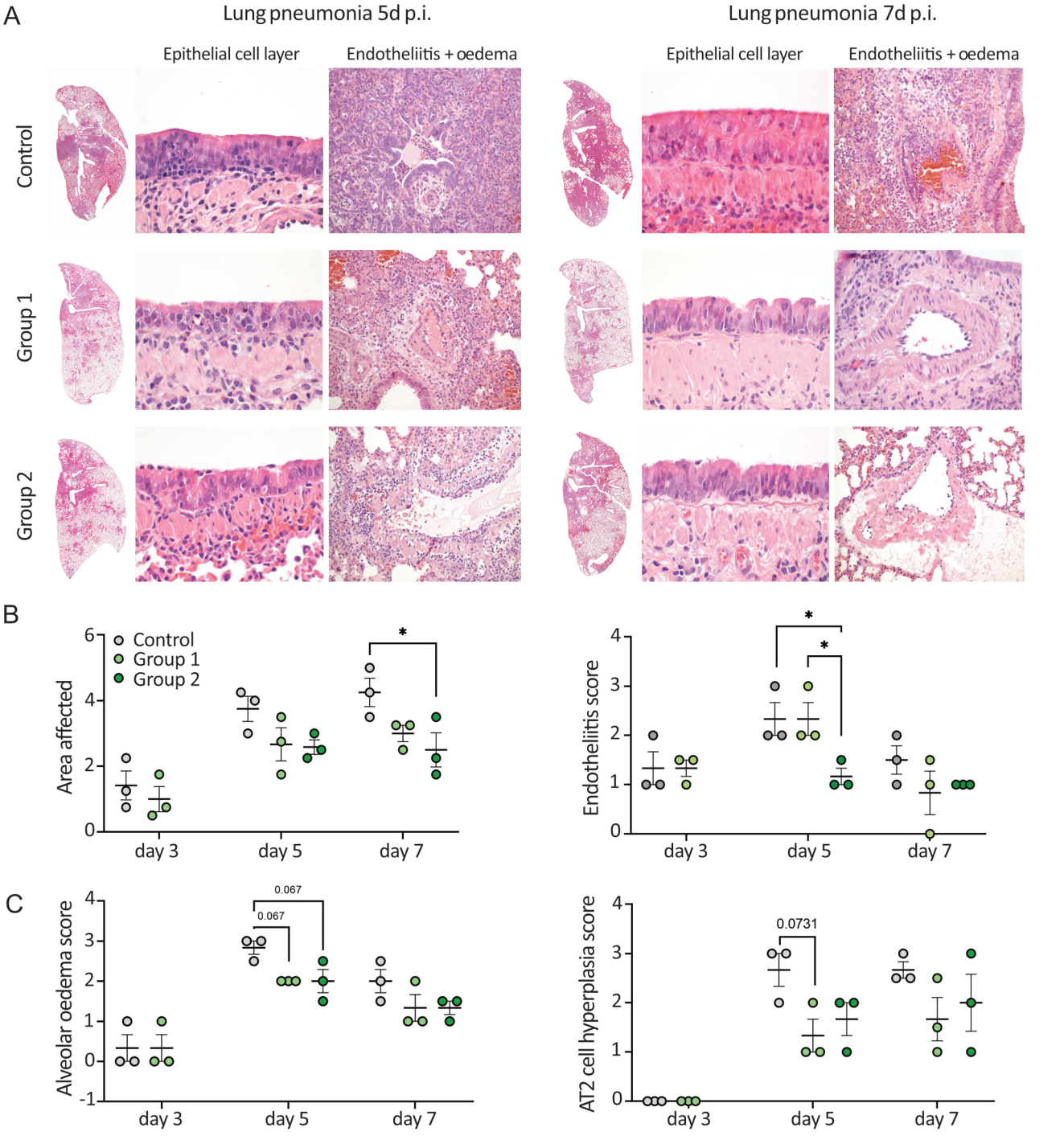

Figure 3 Lung tissue pathology scores are reduced in infected hamsters after treatment with STA-9090. Longitudinal sections of left lungs from Syrian hamsters after 5 days or 7 days infection with SARS-CoV-2 and receiving treatment of STA-9090. Treatment was performed at day 0 p.i. or at day 0 and again at day 4 p.i. and lung tissue was stained with H&E for histological comparisons (A). Shown are whole lung sections and magnification of the epithelial or endothelial layers. Lung pneumonia with oedema formation is seen in darker colours, due to the accumulation of fluids and cells. Representative histology is shown. Semiquantitative analysis of histological lesions quantified at days 3, 5 and 7 p.i. were scored and shown for comparisons. Lung affected area (B), alveolar oedema and AT2 cell hyperplasia (C) and lung endotheliitis (D) are shown. Results are displayed as mean±SE and n=3. Comparisons were made by a one-way ANOVA test. *p<0.05. ANOVA, analysis of variance.

infection was reduced with the treatment at 48 hours p.i., compared with control, with decreased oedema formation, epithelial and endothelial cell damage, and not seen with treatment at 72 h p.i. A significant reduction in the total area affected by pneumonia after treatment was observed at 48 h p.i., comparing to the control group. Alveolar oedema formation was also reduced with treatment at 48 h p.i., but not significantly different to the

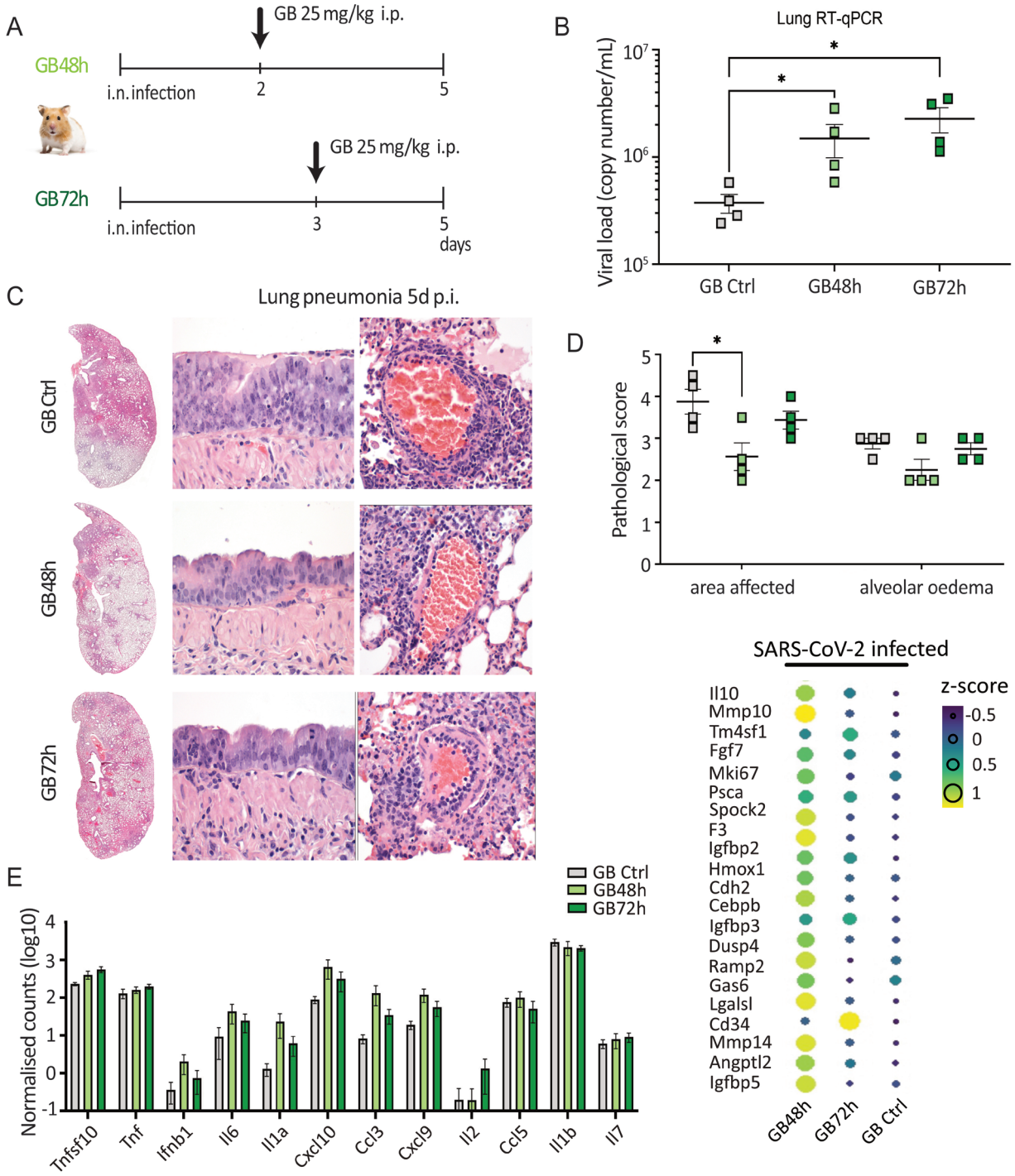

Figure 4 Early treatment with STA-9090 reduces inflammation and lung tissue pathology. (A) Syrian hamsters were challenged with SARS-CoV-2 (1×10^5 PFU) and treated with 25 mg/kg STA-9090 (GB) at 48 h p.i. (GB 48 hours) or at 72 h p.i. (GB 72 hours). Control group received same volume of dilutor and analysis was made at day 5 p.i. (B) RT-qPCR analysis of viral genomic RNA (gRNA) copies detected in homogenised lung tissue was performed at day 5 p.i. (C) Longitudinal sections of left lungs of Syrian hamsters 5 days after infection with SARS-CoV-2 were stained with H&E for histological comparisons. Shown are whole lung sections, and sections focusing on epithelial cell layer and interstitial space. Lung pneumonia with oedema formation is seen in darker colours. Representative histology is shown. (D) Semiquantitative analysis of histological lesions quantified at day 5 p.i. were scored and shown for comparisons for lung affected area and alveolar oedema. Shown is the comparison between the groups receiving STA-9090 at day 2 or 3 p.i. and the control group. (E) Expression analysis of selected genes affected by infection and treatment with STA-9090 in blood samples of Syrian hamsters. Normalised expression values of selected cytokines are shown in logarithmic scale (left) and expression of genes related to tissue regeneration and repair are shown with z-score values of DESeq2 normalised counts (right). Size of the circle and colours show differentiated expression. Average values±SE are shown and n=4. Comparisons were made with a two-tailed Mann-Whitney test (B) and a one-way ANOVA test (D, E). *p<0.05. ANOVA, analysis of variance.

control group (figure 4D). Alveolar epithelial necrosis, bronchitis and broncho-epithelial hyperplasia, immune cell infiltration, perivascular oedema formation and inflammation, AT2 cell hyperplasia and endotheliitis (online supplemental figure 3D) were not affected by the treatment with STA-9090, with only an overall tendency in reduction seen after treatment. To have a deeper understanding of the effects of STA-9090 systemically, we performed total RNA sequencing of whole blood samples. A tendency in increased expression of inflammatory markers, including cytokines, as IL-1b, IL-6 TNFSF10, CXCL10 and CXCL5, and genes related to the IFN signalling was observed in the infected group receiving treatment, when comparing to the mock-treated group. However, these differences were not statistically significant (figure 4E). We then analysed expression of genes related to regeneration of the lung after damage, such as AT2-regenerative genes and anti-inflammatory cytokines, which could possibly explain the reduction in tissue pathology observed by histology. The restoration of the lung tissue homoeostasis after injury is promoted by various cell types, including tissue-resident macrophages and regenerative AT2 cells.[49–52] Their regenerative functions are provided by the release of specific mediators of tissue injury resolution, such as resolvins, protectins or anti-inflammatory cytokines and by the uptake of cell debris.[53–57] The expression of markers related to this regenerative state of the tissue, including Sirpa, Bndf, Mki67, Psca, Krt8, Igfbp3-5, Ramp2, Mmp14 and Gas6, and anti-inflammatory markers, including Il10, Hmox1 and Dusp4, was increased within the animals receiving HSP90 inhibitor, comparing to control, particularly among animals treated at 48 h p.i.

DISCUSSION

SARS-CoV-2 still causes significant outbreaks globally, as new variants appear regularly and vaccination uptakes around the globe are insufficient.[1] Aiming at protecting patients who may develop severe cases of the disease, different treatment strategies that reduce both viral titers and the systemic inflammation taking place after infection are urgently required. Here, we demonstrate the positive effects of STA-9090, an HSP90 inhibitor, in reducing SARS-CoV-2 titers on AEC cells and its tissue protective properties in a hamster model of SARS-CoV-2 infection. In vitro, STA-9090 reduced viral loads in AECs and led to a reduced expression of proinflammatory cytokines on AECs and alveolar macrophages. In vivo, though STA-9090 had no antiviral and anti-inflammatory capacities, lung tissue inflammation, oedema formation and lung epithelial cell damage were globally reduced after treatment, possibly indicating protective properties of STA-9090 in the treatment of COVID-19.

Many viruses were shown to be highly dependent on HSP90 for replication, depending on this chaperone for proper folding and function of the newly rapidly synthesised viral proteins.[25 29] Similar to virus-infected cells, highly proliferative cancer cells also depend on HSP90 to grow. The use of HSP90 inhibitors is, therefore, known in advanced clinical trials for the treatment of some specific tumours, showing no or reduced signs of cytotoxic.[18 22 43] Targeting HSP90 during SARS-CoV-2 infection leads to an inhibition in virion production, as well as reduction in inflammation.[31] Here, HSP90 inhibition was efficient in reducing viral loads in AECs infected with SARS-CoV-2, with concentrations above 100 nM. Contrarily to AECs, we did not observe a reduction in viral loads in infected hamsters after treatment with STA-9090. Interestingly, the concentration of STA-9090 achieved in serum and lung tissue of hamsters 1-day postapplication was approximately 10 nM, with reduced levels at later time points. This concentration is comparable to the lowest doses analysed in vitro, which had no antiviral effect on AECs.

The pleiotropic effects of HSP90 include degradation of distinct proteins, including MAPK, JAK/STAT and NF-kB, affecting distinct signalling pathways implicated in inflammation, cell proliferation and fibrogenesis.[16 58] SARS-CoV-2 infection leads to the activation of the IKK, STAT3 and AKT, which activate NF-kB and lead to inflammation.[20 21 26] Production of proinflammatory cytokines, such as IL-1β, IL-6, CXCL10 and TNF, correlated to the progression of COVID-19, were shown to be reduced by HSP90 inhibition, probably due to the role of HSP90 in the NF-kB activation.[33] A reduced inflammation of the lungs also influences the recruitment and activation of important immune cells, which may contribute to tissue damage.[24 30 36] IFN signalling was shown to have a pivotal role in COVID-19 by coordinating an appropriate inflammatory response against viral infection and the subsequent activation of the innate and adaptive immune response.[59] Here, we also show that STA-9090 could abrogate NF-kB signalling, with a reduction in the expression of NFKBIA on infected cells. STA-9090 also dampened the production of important cytokines and genes involved in IFN signalling in vitro after infection. In vivo, we could not observe the same reduction in the expression of inflammatory markers on treatment, as observed in vitro. This could be a consequence of the low systemic concentrations of the inhibitor, as measured by mass spectrometry. The tissue protective functions of STA-9090 observed in histology might, therefore, be a result of other factors. On lung tissue infection with SARS-CoV-2, a regenerative process with induction of AT2 cell proliferation takes place, leading to the repair of tissue damage.[49–52 56 57] Here, the expression of distinct markers that could indicate this regenerative state was upregulated among animals treated with STA-9090. Treatment with STA-9090 had probably contributed to an improved epithelial regeneration after tissue injury. Moreover, Hub genes involved in angiogenesis and tissue repair, including Pde5a, Cdh2 and Angpt1, are enhanced on Hmox1 and Il10 expression, further contributing to this protective role.[57] Here, expression of anti-inflammatory markers and genes related to tissue homoeostasis were overall increased among animals treated at 48 h p.i. and

could have further improved tissue repair. Activation of anti-inflammatory and regenerative cells could be possibly responsible for the improvement in tissue pathology seen in the animals after treatment and should, therefore, be further investigated. However, analysis of blood transcriptome to understand lung tissue regeneration should be carefully interpreted. HSP90 inhibition was shown to attenuate the reduction of intercellular junction proteins, as occluding and VE-cadherin, activated by SARS-CoV-2 spike protein, protecting against vascular permeability.[10] We could also observe a protective role of STA-9090 on the endothelial cell layer, as seen by reduced lung tissue endotheliitis. This is in agreement with other studies that show a protective role of HSP90 inhibition in barrier dysfunction.[30] However, a late application of STA-9090 was not sufficient to protect animals from disease. Probably, a delayed application of STA-9090, combined with an increase in viral load had the opposite effect to what was expected, with increased and prolonged inflammation of the tissue. Therefore, the efficacy of STA-9090 in reducing tissue inflammation and tissue pathology are dependent on the frequency and timing of the administration of this inhibitor. In vivo, even if not sufficient to block viral replication, the reduced concentrations of STA-9090 achieved systemically could be sufficient to provide protective functions to the tissue against the infection.

Our study has several limitations. The mass spectrometry data indicated that the concentrations of the inhibitor reached in the lung tissue and serum of hamsters was likely not high enough to lead to the antiviral and anti-inflammatory properties of STA-9090, seen in vitro. Still, we were able to see a reduction in lung tissue pathology, with reduced inflammation and endothelial cell damage. Increasing the concentration of STA-9090, by, for example, intravenous application, instead of i.p., as performed for the hamsters, could increase its antiviral and anti-inflammatory capacities. Also, applying the medicine directly into the lungs by inhalation could be an interesting approach to enhance its concentrations locally, thereby improving tissue protection. Moreover, the low number of animals, as well as mixing male and female animals in the groups, led to increased variability in the results, with increased standard errors. Different responses to infection between sex are already known and were described elsewhere. Future studies should increase the number of animals tested or focus distinctively on the sex of the animals used, to better understand the mechanisms of action of STA-9090 in reducing tissue pathology in COVID-19 or other inflammatory diseases of the lung.

Altogether, we describe here the distinct beneficial properties of STA-9090 in controlling cellular activation and tissue inflammation, and in this line, contributing to tissue protection in COVID-19. We postulate that in future experiments, a combinatory strategy of treatment with STA-9090 and different antiviral compounds could be beneficial in moderate and severe cases of the disease, where STA-9090 would promote stabilisation of the endothelial barrier of the lung, diminish inflammation and promote tissue protection, while reduced viral replication would lead to improvements in the disease outcome.

Author affiliations
[1]RNA Biology and Posttranscriptional Regulation, Max Delbruck Centre for Molecular Medicine in the Helmholtz Association, Berlin, Germany
[2]Corporate Member of Freie Universität Berlin und Humboldt-Universität zu Berlin, Department of Infectious Diseases, Respiratory Medicine and Critical Care, Charité Universitätsmedizin Berlin, Berlin, Germany
[3]Institute of Virology, Free University of Berlin, Berlin, Germany
[4]Research Unit Analytical Pathology, Helmholtz Zentrum Munchen Deutsches Forschungszentrum fur Gesundheit und Umwelt, Neuherberg, Germany
[5]Department of Veterinary Pathology, Free University of Berlin, Berlin, Germany
[6]Proteomics and Metabolomics, Max Delbruck Centre for Molecular Medicine in the Helmholtz Association, Berlin, Germany
[7]Institute for Biology, Humboldt-Universitat zu Berlin, Berlin, Germany

Contributors Conceptualisation of the manuscript was done by ML, EW, JT, SK, ADG and ACH. Development of the experiments and analysis was done by LGTA, MB, CL, MF, JB, TCF, JMA, GM, JG and KH. Writing was done by LGTA and EW, and review performed by all authors. LGTA is guarantor of this study.

Funding We thank the support of Jeannine Wilde and Madlen Sohn from the BIH/MDC Genomics Technology platform in Berlin for the sequencing. LGTA, EW and ML are supported by the Project 'Virological and immunological determinants of COVID-19 pathogenesis–lessons to get prepared for future pandemics (KA1-Co-02 'COVIPA')', a grant from the Helmholtz Association Initiative and Networking Fund. ACH was supported by BMBF (RAPID). KH, ADG and ACH were funded by BMBF (NUM-COVID 19, Organo-Strat 01KX2021), Charite 3^{R}, Einstein Foundation EC3R and by DFG (SFB-TR84)

Competing interests None declared.

Patient and public involvement Patients and/or the public were not involved in the design, or conduct, or reporting, or dissemination plans of this research.

Patient consent for publication Not applicable.

Ethics approval Experiments with Syrian hamsters (Mesocricetus auratus; breed RjHan:AURA, JanvierLabs, France) were approved by the relevant state authority (LaGeSo–Berlin, Germany, under the approval number G 0086/20) and executed in compliance with (inter)national regulations. Studies with human cells were approved by the local ethics committee (project EA2/079/13, Ethics committee of the Charité Universitätsmedizin–Berlin, Germany).

Provenance and peer review Not commissioned; externally peer reviewed.

Data availability statement Data are available in a public, open access repository. Raw sequencing data, count table for normalised and non-normalised data for the bulk RNAsequencing experiments are available at the Gene Expression Omnibus database (GEO), under theidentifier GSE227846 (GEO: https://www.ncbi.nlm.nih.gov/geo/query/acc.cgi?acc=GSE227846).

ORCID iD
Luiz Gustavo Teixeira Alves http://orcid.org/0000-0002-5822-4168

REFERENCES

1 WHO. Coronavirus disease (COVID-19) pandemic, . 2021.Available: https://www.who.int/emergencies/diseases/novel-coronavirus-2019
2 Wu F, Zhao S, Yu B, *et al*. A new Coronavirus associated with human respiratory disease in China. *Nature* 2020;579:265–9.
3 Wu Z, McGoogan JM. Characteristics of and important lessons from the Coronavirus disease 2019 (COVID-19) outbreak in China. *JAMA* 2020;323:1239.
4 Osuchowski MF, Winkler MS, Skirecki T, *et al*. The COVID-19 puzzle: Deciphering pathophysiology and phenotypes of a new disease entity. *Lancet Respir Med* 2021;9:622–42.
5 Liao M, Liu Y, Yuan J, *et al*. Single-cell landscape of Bronchoalveolar immune cells in patients with COVID-19. *Nat Med* 2020;26:842–4.
6 Blanco-Melo D, Nilsson-Payant BE, Liu W-C, *et al*. Imbalanced host response to SARS-Cov-2 drives development of COVID-19. *Cell* 2020;181:1036–45.
7 Apicella M, Campopiano MC, Mantuano M, *et al*. COVID-19 in people with diabetes: understanding the reasons for worse outcomes. *Lancet Diabetes Endocrinol* 2020;8:782–92.
8 Hoffmann M, Kleine-Weber H, Schroeder S, *et al*. SARS-Cov-2 cell entry depends on Ace2 and Tmprss2 and is blocked by a clinically proven protease inhibitor. *Cell* 2020;181:271–80.
9 Schimmel L, Chew KY, Stocks CJ, *et al*. Endothelial cells are not Productively infected by SARS-Cov-2. *Clin Transl Immunology* 2021;10:e1350.
10 Colunga Biancatelli RML, Solopov PA, Gregory B, *et al*. Hsp90 inhibitors modulate SARS-Cov-2 spike protein subunit 1-induced human pulmonary Microvascular endothelial activation and barrier dysfunction. *Front Physiol* 2022;13:812199.
11 Deinhardt-Emmer S, Böttcher S, Häring C, *et al*. SARS-Cov-2 causes severe epithelial inflammation and barrier dysfunction. *J Virol* 2021;95.
12 Guimarães PO, Quirk D, Furtado RH, *et al*. Tofacitinib in patients hospitalized with COVID-19 pneumonia. *N Engl J Med* 2021;385:406–15.
13 Patel J, Bass D, Beishuizen A, *et al*. A randomized trial of anti-GM-CSF Otilimab in severe COVID-19 pneumonia (OSCAR). *Eur Respir J* 2023;61:2101870.
14 Sterne JAC, Murthy S, Diaz JV, *et al*. Association between administration of systemic corticosteroids and mortality among critically ill patients with COVID-19. *JAMA* 2020;324:1330–41.
15 RECOVERY Collaborative Group, Horby P, Lim WS, *et al*. Dexamethasone in hospitalized patients with COVID-19. *N Engl J Med* 2021;384:693–704.
16 Colunga Biancatelli RML, Solopov P, Gregory B, *et al*. Hsp90 inhibition and modulation of the Proteome: Therapeutical implications for idiopathic pulmonary fibrosis (IPF). *Int J Mol Sci* 2020;21:5286.
17 Saibil H. Chaperone machines for protein folding, unfolding and Disaggregation. *Nat Rev Mol Cell Biol* 2013;14:630–42.
18 Garcia-Carbonero R, Carnero A, Paz-Ares L. Inhibition of Hsp90 molecular Chaperones: moving into the clinic. *Lancet Oncol* 2013;14:S1470-2045(13)70169-4:e358–69.:.
19 Mahalingam D, Swords R, Carew JS, *et al*. Targeting Hsp90 for cancer therapy. *Br J Cancer* 2009;100:1523–9.
20 Tudas RA, Gannon RM, Thurman AL, *et al*. HSP90 inhibition modulates nfκb signaling in airway goblet cell metaplasia. *Cell Biology* [Preprint].
21 Lawrence T. The nuclear factor NF-kappaB pathway in inflammation. *Cold Spring Harb Perspect Biol* 2009;1:a001651.
22 Soga S, Akinaga S, Shiotsu Y. Hsp90 inhibitors as anti-cancer agents, from basic discoveries to clinical development. *Curr Pharm Des* 2013;19:366–76.
23 Lackie RE, Maciejewski A, Ostapchenko VG, *et al*. The Hsp70/Hsp90 chaperone machinery in neurodegenerative diseases. *Front Neurosci* 2017;11:254.
24 Tukaj S, Węgrzyn G. Anti-Hsp90 therapy in autoimmune and inflammatory diseases: a review of Preclinical studies. *Cell Stress Chaperones* 2016;21:213–8.
25 Geller R, Taguwa S, Frydman J. Broad action of hsp90 as a host chaperone required for viral replication. *Biochimica et Biophysica Acta (BBA) - Molecular Cell Research* 2012;1823:698–706.
26 Thangjam GS, Birmpas C, Barabutis N, *et al*. Hsp90 inhibition suppresses NF-ΚB transcriptional activation via Sirt-2 in human lung Microvascular endothelial cells. *Am J Physiol Lung Cell Mol Physiol* 2016;310:L964–74.
27 Joshi AD, Dimitropoulou C, Thangjam G, *et al*. Heat shock protein 90 inhibitors prevent LPS-induced endothelial barrier dysfunction by disrupting Rhoa signaling. *Am J Respir Cell Mol Biol* 2014;50:170–9.
28 Dong H-M, Le Y-Q, Wang Y-H, *et al*. Extracellular heat shock protein 90A mediates HDM-induced bronchial epithelial barrier dysfunction by activating Rhoa/MLC signaling. *Respir Res* 2017;18:111.
29 Gao J, Xiao S, Liu X, *et al*. Inhibition of Hsp90 attenuates porcine reproductive and respiratory syndrome virus production in vitro. *Virol J* 2014;11:17.
30 Antonov A, Snead C, Gorshkov B, *et al*. Heat shock protein 90 inhibitors protect and restore pulmonary endothelial barrier function. *Am J Respir Cell Mol Biol* 2008;39:551–9.
31 Zhao Z, Xu L-D, Zhang F, *et al*. Heat shock protein 90 facilitates SARS-Cov-2 structural protein-mediated Virion assembly and promotes virus-induced Pyroptosis. *Journal of Biological Chemistry* 2023;299:104668.
32 Shatzer A, Ali MA, Chavez M, *et al*. Ganetespib, an Hsp90 inhibitor, kills Epstein–Barr virus (EBV)-Infected B and T cells and reduces the percentage of EBV-infected cells in the blood. *Leukemia & Lymphoma* 2017;58:923–31.
33 Wyler E, Mösbauer K, Franke V, *et al*. Transcriptomic profiling of SARS-Cov-2 infected human cell lines identifies Hsp90 as target for COVID-19 therapy. *iScience* 2021;24:102151.
34 Li C, Chu H, Liu X, *et al*. Human Coronavirus dependency on host heat shock protein 90 reveals an antiviral target. *Emerging Microbes & Infections* 2020;9:2663–72.
35 Makhoba XH, Makumire S. The capture of host cell's resources: the role of heat shock proteins and Polyamines in SARS-COV-2 (COVID-19) pathway to viral infection. *Biomol Concepts* 2022;13:220–9.
36 Goswami R, Russell VS, Tu JJ, *et al*. Oral Hsp90 inhibitor SNX-5422 attenuates SARS-Cov-2 replication and Dampens inflammation in airway cells. *iScience* 2021;24:103412.
37 Nouailles G, Wyler E, Pennitz P, *et al*. Temporal Omics analysis in Syrian Hamsters unravel cellular Effector responses to moderate COVID-19. *Nat Commun* 2021;12:4869.
38 Vinzing M, Eitel J, Lippmann J, *et al*. NAIP and Ipaf control Legionella Pneumophila replication in human cells. *J Immunol* 2008;180:6808–15.
39 Kim D, Paggi JM, Park C, *et al*. Graph-based genome alignment and Genotyping with Hisat2 and HISAT-genotype. *Nat Biotechnol* 2019;37:907–15.
40 Liao Y, Smyth GK, Shi W. The R package Rsubread is easier, faster, cheaper and better for alignment and Quantification of RNA sequencing reads. *Nucleic Acids Res* 2019;47:e47.
41 Love MI, Huber W, Anders S. Moderated estimation of fold change and dispersion for RNA-Seq data with Deseq2. *Genome Biol* 2014;15:550.
42 Lubkowska A, Pluta W, Strońska A, *et al*. Role of heat shock proteins (Hsp70 and Hsp90) in viral infection. *Int J Mol Sci* 2021;22:9366.
43 Okamoto T, Nishimura Y, Ichimura T, *et al*. Hepatitis C virus RNA replication is regulated by Fkbp8 and Hsp90. *EMBO J* 2006;25:5015–25.
44 Goldman JW, Raju RN, Gordon GA, *et al*. A first in human, safety, pharmacokinetics, and clinical activity phase I study of once weekly administration of the Hsp90 inhibitor Ganetespib (STA-9090) in patients with solid malignancies. *BMC Cancer* 2013;13:152.
45 Guan L, Zou Q, Liu Q, *et al*. Hsp90 inhibitor Ganetespib (STA-9090) inhibits tumor growth in C-Myc-dependent Esophageal squamous cell carcinoma
46 Neufeldt CJ, Cerikan B, Cortese M, *et al*. SARS-Cov-2 infection induces a pro-inflammatory cytokine response through cGAS-STING and NF-ΚB. *Commun Biol* 2022;5:45.
47 D'Alessio FR, Heller NM. COVID-19 and myeloid cells: complex interplay correlates with lung severity. *J Clin Invest* 2020;130:6214–7.
48 Hönzke K, Obermayer B, Mache C, *et al*. Human lungs show limited Permissiveness for SARS-Cov-2 due to scarce Ace2 levels but virus-induced expansion of inflammatory Macrophages. *Eur Respir J* 2022;60:2102725.
49 Paris AJ, Hayer KE, Oved JH, *et al*. Stat3-BDNF-Trkb signalling promotes alveolar epithelial regeneration after lung injury. *Nat Cell Biol* 2020;22:1197–210.
50 Choi J, Park J-E, Tsagkogeorga G, *et al*. Inflammatory signals induce At2 cell-derived damage-associated transient progenitors that mediate alveolar regeneration. *Cell Stem Cell* 2020;27:366–82.
51 Strunz M, Simon LM, Ansari M, *et al*. Longitudinal single cell transcriptomics reveals krt8+ alveolar epithelial progenitors in lung regeneration. *Systems Biology* [Preprint].
52 Zhao F, Ma Q, Yue Q, *et al*. SARS-Cov-2 infection and lung regeneration. *Clin Microbiol Rev* 2022;35:e00188-21.

53 Davey A, McAuley DF, O'Kane CM. Matrix Metalloproteinases in acute lung injury: mediators of injury and drivers of repair. *Eur Respir J* 2011;38:959–70.
54 Herold S, Mayer K, Lohmeyer J. Acute lung injury: how Macrophages Orchestrate resolution of inflammation and tissue repair. *Front Immunol* 2011;2:65.
55 Han W, Tanjore H, Liu Y, *et al*. Identification and characterization of alveolar and recruited lung Macrophages during acute lung inflammation. *J Immunol* 2023;210:1827–36.
56 Gill SE, Huizar I, Bench EM, *et al*. Tissue inhibitor of Metalloproteinases 3 regulates resolution of inflammation following acute lung injury. *Am J Pathol* 2010;176:64–73.
57 Sun Z, Chen A, Fang H, *et al*. B cell-derived IL-10 promotes the resolution of Lipopolysaccharide-induced acute lung injury. *Cell Death Dis* 2023;14:418.
58 Schumacher JA, Crockett DK, Elenitoba-Johnson KSJ, *et al*. Proteome-wide changes induced by the Hsp90 inhibitor, Geldanamycin in Anaplastic large cell lymphoma cells. *Proteomics* 2007;7:2603–16.
59 Ye L, Schnepf D, Staeheli P. Interferon-Λ Orchestrates innate and adaptive Mucosal immune responses. *Nat Rev Immunol* 2019;19:614–25.
60 Winkler ES, Bailey AL, Kafai NM, *et al*. SARS-Cov-2 infection of human Ace2-transgenic mice causes severe lung inflammation and impaired function. *Nat Immunol* 2020;21:1327–35.

Supplemental Figures and Table

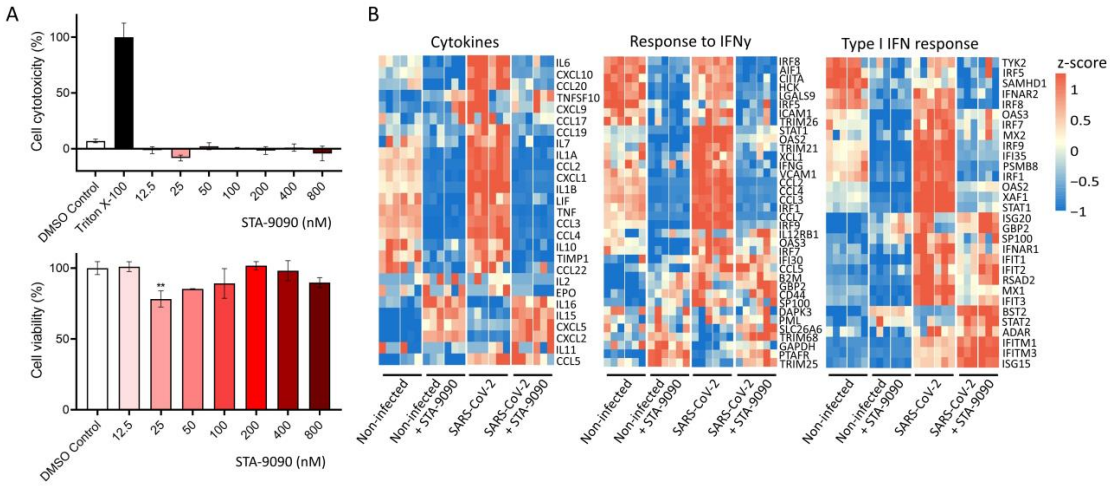

Supplemental figure 1 Anti-inflammatory properties of STA-9090**.** AECs and alveolar macrophages were isolated from human lung tissue and cultured in medium prior to the treatment with the HSP90 inhibitor STA-9090. (A) Cytotoxicity (up) and viability (down) tests were performed with AECs to evaluate the effects of STA-9090 on the cells. (B) Heatmaps of differently expressed genes in alveolar macrophages after infection with SARS-CoV-2 and treatment with 100 nM of STA-9090. Non-infected cells, with or without treatment, serve as control. Cytokines, genes related to cellular response to IFNγ and type I IFN response pathway were selected, as previously described.[60] Columns represent samples and rows genes. Shown are z-scores of DESeq2-normalised data from 2 donors, analysed independently, and color scale ranges from blue (10 % lower quantile) to red (10 % upper quantile) of the selected genes. N=3 in A and n=2 in B. Unpaired t-test used for comparison in A. **p<0.01. AECs, alveolar epithelial cells.

Table 1 Animal cohort information. Sex of animals used for both *in vivo* experiments in the respective groups analysed**.**

	Experiment 1									Experiment 2		
	Control			Group1			Group2			Control	GB 48h	GB 72h
Days p.i.	**3**	**5**	**7**	**3**	**5**	**7**	**3**	**5**	**7**	**5**	**5**	**5**
Male	2	1	2	1	2	1	-	1	2	2	2	2
Female	1	2	1	2	1	2	-	2	1	2	2	2

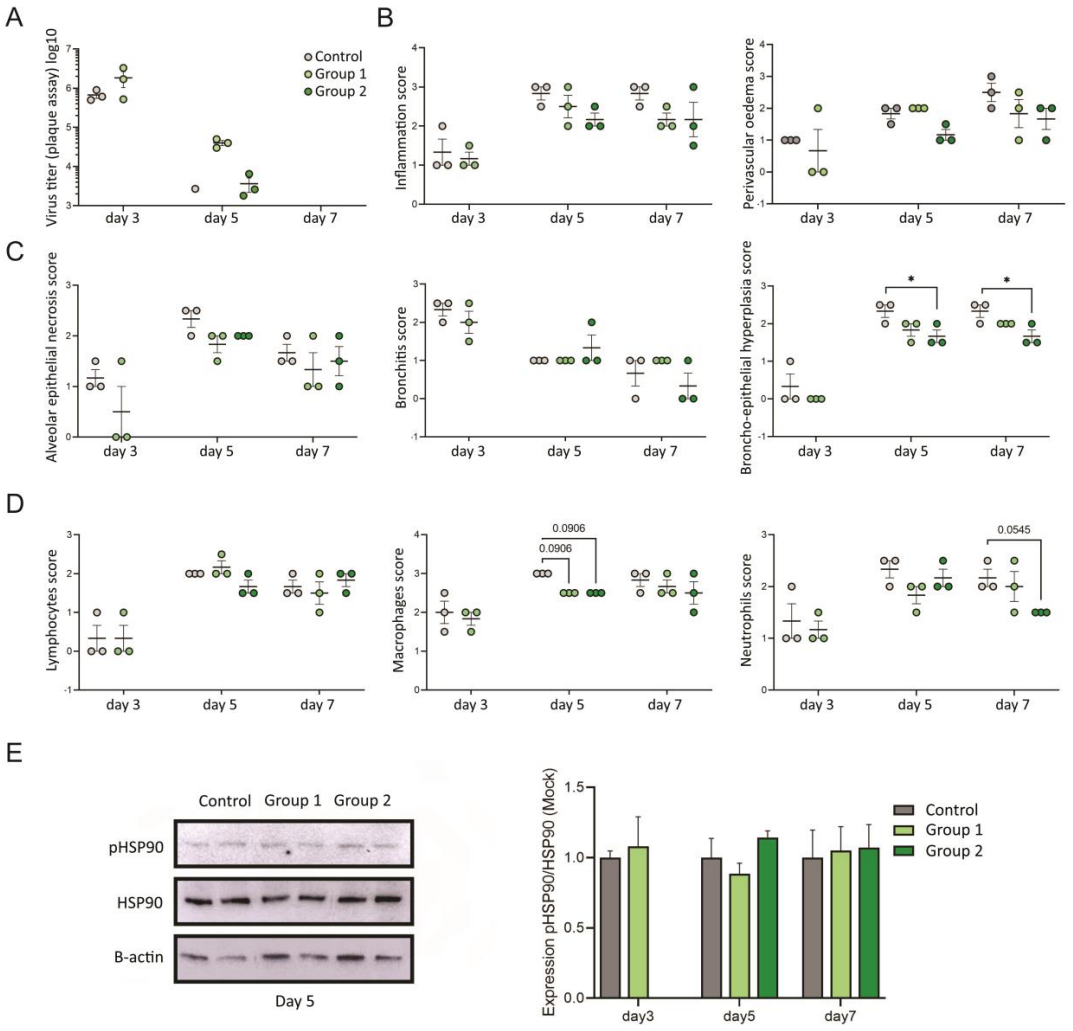

Supplemental figure 2 Lung tissue pathology scoring is improved after treatment with STA-9090. (A) Quantification of replicating competent virus as plaque-forming units (PFU) per gram homogenised lung tissue. Longitudinal sections of left lungs from Syrian hamsters infected with SARS-CoV-2 and treated with STA-9090 at day 0 (Group 1) or day 0 + 4 (Group 2) p.i. were evaluated after 3-, 5- or 7-days infection by a semi-quantitative pathological scoring. Shown are scores for inflammation and perivascular oedema (B), alveolar epithelial necrosis, bronchitis, broncho-epithelial cell hyperplasia (C), and infiltration of lymphocytes, macrophages and neutrophils (D). (E) Western blot for phospho-HSP90 and HSP90 from lung tissue homogenate at day 5 after infection with SARS-CoV-2 and treatment with STA-9090 (left). β-actin was used as internal control for normalisation and ratio between phospho-HSP90 and HSP90 expression was analysed by comparison to the Mock treated group (right). Results are displayed as mean ± SE and n=3. Comparisons were made with a two-Way ANOVA test. *p<0.05. ANOVA, analysis of variance.

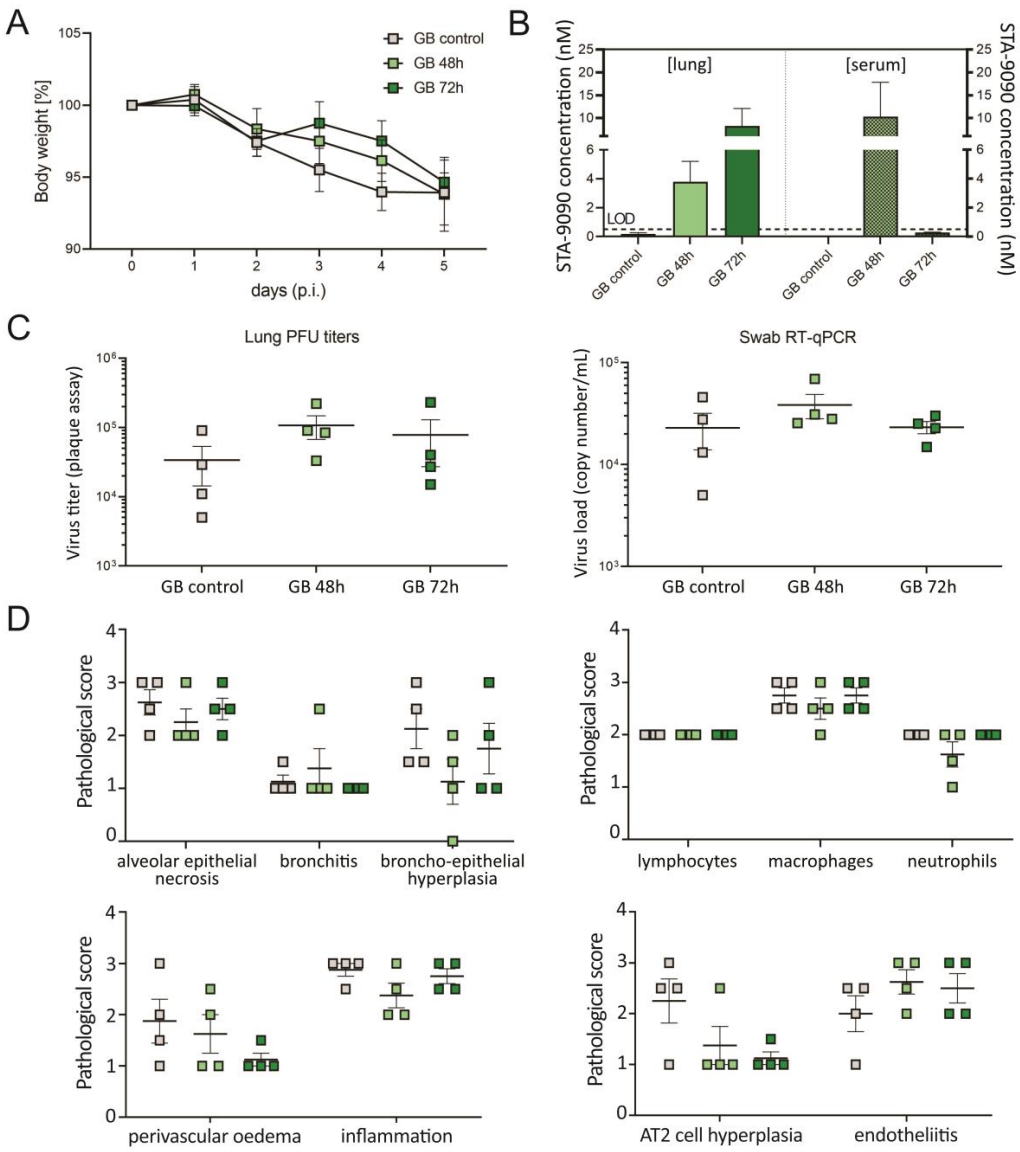

Supplemental figure 3 Early treatment with STA-9090 reduces inflammation in the lungs of SARS-CoV-2 infected-hamsters. Syrian hamsters were challenged with SARS-CoV-2 (1 x 10^5 PFU) and treated with 25 mg/kg STA-9090 (GB) at 48 h p.i. (GB 48h) or at 72 h p.i. (GB 72h). Control group received same volume of dilutor and analysis was made at day 5 p.i. (A) Body weight in percentage from the original weight was measured daily after infection of the animals with SARS-CoV-2. (B) Pharmacokinetics of STA-9090 quantified by mass spectrometry in the lung tissue (left) or serum (right) of Syrian hamsters after 3 (GB 48h) or 2 days (GB 72h) treatment. Concentrations are shown in nM. (C) Quantification of replication competent virus as plaque-forming units (PFU) per gram homogenised lung tissue was analysed for viral

titers. RT-qPCR analysis of viral genomic RNA (gRNA) copies detected in oropharyngeal swabs at day 5 p.i. (D) Semi-quantitative analysis of histological sections of the left lungs from hamsters analysed after 5 days infection were compared for the pathological score of alveolar epithelial necrosis, bronchitis, broncho-epithelial cell hyperplasia, immune cell infiltration, perivascular oedema, inflammation score, AT2 cell hyperplasia and endotheliitis, as shown. Results are displayed as mean ± SE and n=4. LOD, limit of detection

ICMJE DISCLOSURE FORM

Date: 4/12/2023

Your Name: Luiz Gustavo Teixeira Alves

Manuscript Title: Ganetespib as a potential therapeutic option for moderate to severe COVID-19 cases

Manuscript Number (if known): Click or tap here to enter text.

In the interest of transparency, we ask you to disclose all relationships/activities/interests listed below that are related to the content of your manuscript. "Related" means any relation with for-profit or not-for-profit third parties whose interests may be affected by the content of the manuscript. Disclosure represents a commitment to transparency and does not necessarily indicate a bias. If you are in doubt about whether to list a relationship/activity/interest, it is preferable that you do so.

The author's relationships/activities/interests should be defined broadly. For example, if your manuscript pertains to the epidemiology of hypertension, you should declare all relationships with manufacturers of antihypertensive medication, even if that medication is not mentioned in the manuscript.

In item #1 below, report all support for the work reported in this manuscript without time limit. For all other items, the time frame for disclosure is the past 36 months.

		Name all entities with whom you have this relationship or indicate none (add rows as needed)	**Specifications/Comments (e.g., if payments were made to you or to your institution)**
Time frame: Since the initial planning of the work			
1	All support for the present manuscript (e.g., funding, provision of study materials, medical writing, article processing charges, etc.) **No time limit for this item.**	☐ None	
		Aldeyra Therapeutics	Provided the HSP90 inhibitor Ganetespib, tested in the study, through a formal MTA
			Click the tab key to add additional rows.
Time frame: past 36 months			
2	Grants or contracts from any entity (if not indicated in item #1 above).	☐ **None**	
		Project "Virological and immunological determinants of COVID-19 pathogenesis – lessons to get prepared for future pandemics (KA1-Co-02 'COVIPA')", a grant from the Helmholtz Association Initiative and Networking Fund.	

		Name all entities with whom you have this relationship or indicate none (add rows as needed)	Specifications/Comments (e.g., if payments were made to you or to your institution)
3	Royalties or licenses	☒ **None**	
4	Consulting fees	☒ **None**	
5	Payment or honoraria for lectures, presentations, speakers bureaus, manuscript writing or educational events	☒ **None**	
6	Payment for expert testimony	☒ **None**	
7	Support for attending meetings and/or travel	☒ **None**	
8	Patents planned, issued or pending	☒ **None**	
9	Participation on a Data Safety	☒ **None**	

		Name all entities with whom you have this relationship or indicate none (add rows as needed)	Specifications/Comments (e.g., if payments were made to you or to your institution)
	Monitoring Board or Advisory Board		
10	Leadership or fiduciary role in other board, society, committee or advocacy group, paid or unpaid	☒ **None**	
11	Stock or stock options	☒ **None**	
12	Receipt of equipment, materials, drugs, medical writing, gifts or other services	☐ **None**	
13	Other financial or non-financial interests	☒ **None**	

Please place an "X" next to the following statement to indicate your agreement:

☒ I certify that I have answered every question and have not altered the wording of any of the questions on this form.

The ARRIVE Essential 10: Compliance Questionnaire

Use this questionnaire to evaluate how well a manuscript complies with the ARRIVE Essential 10. It can be applied to any manuscript describing comparative experiments in living animals, by assessors such as journal staff, editors, or peer reviewers.

	Item	Question(s)	Answers
1	Study Design	Are all experimental and control groups clearly identified?	☐ Yes, for at least one experiment ☐ No
		Is the experimental unit (e.g. an animal, litter or cage of animals) clearly identified?	☐ Yes, for at least one experiment ☐ No
2	Sample Size	Is the exact number of experimental units in each group at the start of the study provided (e.g. in the format '*n*=')?	☐ Yes, for at least one experiment ☐ No
		Is the method by which the sample size was chosen explained?	☐ Yes, for at least one experiment ☐ No
3	Inclusion & Exclusion Criteria	Are the criteria used for including and excluding animals, experimental units, or data points provided?	☐ Yes, for at least one experiment ☐ No
		Are any exclusions of animals, experimental units, or data points reported, or is there a statement indicating that there were no exclusions?	☐ Yes, for at least one analysis ☐ No
4	Randomisation	Is the method by which experimental units were allocated to control and treatment groups described?	☐ Yes, for at least one experiment ☐ No
5	Blinding	Is it clear whether researchers were aware of, or blinded to, the group allocation at any stage of the experiment or data analysis?	☐ Yes, for at least one experiment ☐ No
6	Outcome Measures	For all experimental outcomes presented, are details provided of exactly what parameter was measured?	☐ Yes, for at least one experiment ☐ No
7	Statistical Methods	Is the statistical approach used to analyse each outcome detailed?	☐ Yes, for at least one analysis ☐ No
		Is there a description of any methods used to assess whether data met statistical assumptions?	☐ Yes, for at least one analysis ☐ No ☐ Not applicable
8	Experimental Animals	Are all species of animal used specified?	☐ Yes, for at least one experiment ☐ No
		Is the sex of the animals specified?	☐ Yes, for at least one experiment ☐ No ☐ Not applicable to species
		Is at least one of age, weight or developmental stage of the animals specified?	☐ Yes, for at least one experiment ☐ No
9	Experimental Procedures	Are both the timing and frequency with which procedures took place specified?	☐ Yes, for at least one experiment ☐ No
		Are details of acclimatisation periods to experimental locations provided?	☐ Yes, for at least one experiment ☐ No
10	Results	Are descriptive statistics for each experimental group provided, with a measure of variability (e.g. mean and SD, or median and range)?	☐ Yes, for at least one experiment ☐ No ☐ Not applicable to the type of data collected
		Is the effect size and confidence interval provided?	☐ Yes, for at least one experiment ☐ No ☐ Not applicable to the type of analysis used

Notes on questionnaire design

The ARRIVE guidelines are a useful resource for authors preparing manuscripts describing animal research, and also provide a framework to evaluate the transparency of those manuscripts. To assess reporting quality, numerous studies have in the past sought to operationalise reporting guidelines (including ARRIVE). Typically, this involves scoring a manuscript's degree of compliance with guideline items in a binary fashion (e.g. an item is either not reported or reported) [1-3], a graded fashion (e.g. not, partially, or completely reported) [4,5], or a combination of the two [6].

This questionnaire has been designed to be as concise and user-friendly as possible. The number of questions used to assess a manuscript's compliance has been kept to a minimum, and in most cases each question is designed to be answered in a binary fashion. Compliance with some Essential 10 sub-items is inherently impossible to judge in this way, instead requiring a subjective judgement on the level of detail provided. For this reason, not all sub-items are represented by a question in this questionnaire.

To facilitate binary answers, it has been necessary to identify the minimum information in a manuscript sufficient to comply with each question. The strengths of this approach include the relatively short length of the questionnaire (and the correspondingly low time burden of using it), and the avoidance of ambiguity that would arise from a graded answering system, in which an intermediate score (e.g. 'partially/insufficiently reported') could denote a number of distinct deficiencies in compliance with an item (e.g. either only part of the item was complied with, or only the reporting of some experiments in the manuscript complied with the item.)

Limitations of this approach centre on the necessity to identify the minimum information sufficient to comply with each question. In some cases, this has resulted in questions that require a guideline sub-item's criteria to have been fulfilled in the reporting of only one experiment in a manuscript. As a result, not all experiments in a manuscript may be described in a way that fulfils that criterion, despite the manuscript being considered to comply with the guidelines overall.

References

1. Hair *et al* (2020). *Res Integ Peer Rev*. doi: 10.1186/s41073-019-0069-3
2. Tihanyi *et al* (2019). *J Surg Res*. doi: 10.1016/j.jss.2018.10.038
3. Zhao *et al* (2020). *BMC Vet Res*. doi: 10.1186/s12917-020-02664-1
4. Han *et al* (2017). *Plos One*. doi: 10.1371/journal.pone.0183591
5. Chatzimanouil *et al* (2019). *J Am Soc Nephrol*. doi: 10.1681/ASN.2018050515
6. Leung *et al* (2018). *Plos One*. doi: 10.1371/journal.pone.0197882